The Design of 4×4 Multimode Interference Coupler Based Microring Resonators on an SOI Platform

Trung-Thanh Le and Laurence W. Cahill

Abstract—This paper would like to propose a novel microring resonator based on 4×4 multimode interference (MMI) couplers. The device acts as two separate microring resonators just in one structure. The transfer matrix method and the three dimensional beam propagation method (3D-BPM) are used to verify the working principle of the device. The device is then designed on silicon on insulator (SOI) technology. This device may be a very promising building block for optical switches, filters, add-drop multiplexers, delay lines and modulators.

Keywords— integrated optics, multimode interference couplers, optical logic gates.

1. Introduction

Microring resonators have been used as a basic building block for optical signal processing applications such as optical switches, filters, modulators, and add-drop multiplexers [1]. Almost all of the reported works on microring resonator structures have used directional couplers as the coupling element [2]. In order to meet a variety of requirements for high-speed signal processing, the coupling coefficient needs to be adjusted arbitrarily and the directional couplers can meet this requirement. However, for applications requiring high quality factor Q of the resonators, i.e., for high speed operation, the separations between two waveguides in the directional coupler must be very small. As a result, high loss due to conversion loss of modes is occurred as shown in [3] recently. Moreover, the directional coupler has a large size and small fabrication tolerance. Therefore, multimode interference (MMI) couplers are used in such structures instead of directional couplers due to their advantages of compactness, ease of fabrication, large fabrication tolerance and ease of cascaded integration [4].

A microring resonator based on a 2×2 MMI coupler was demonstrated on silicon on insulator (SOI) channel waveguides for the first time in [2]. However, the coupling ratios of the conventional MMI couplers are very limited and there are only four available coupling ratios 0:100, 50:50, 85:15, and 72:28 if using only one conventional MMI coupler [5]. Therefore, it is highly desired to implement the couplers with variable coupling ratios. To do so, the common approach is to use Mach-Zehnder interferometer (MZI) structures, in which phase shifters are added to the MZI arms to control the phase of the propagation signals as shown in [6], [7].

In this paper, a novel microring resonator based on 4×4 MMI couplers is given for the first time. The most interesting characteristic of the proposed device is that the device acts as two separate microring resonators based on 2×2 MMI couplers. The coupling ratios can be varied by using two separate phase shifters for the two microring resonators. In order to verify the working principle of the device, the transfer matrix and beam propagation method are used. The device is designed on an SOI platform.

2. Microring Resonators Based on 4×4 MMI Couplers

A microring resonator based on 4×4 MMI couplers (MMI-MZI structure) is shown in Fig. 1. The two 4×4 MMI couplers have the same width W_{MMI} and length $L_{MMI} = \frac{3L_\pi}{2}$, where $L_\pi = \frac{\pi}{\beta_0 - \beta_1}$ is the beat length of the MMI coupler. In order to make tunable devices, two phase shifters $\Delta\varphi_1$ and $\Delta\varphi_2$ based on the thermo-optic effect are used in the two arms. Alternatively, passive phase shifters could be used to provide a desired (fixed) power splitting ratio.

In order to analyze the device, the transfer matrix of the identical MMI couplers needs to be derived first and then the total transfer matrix of the device can be determined. The 4×4 MMI coupler can be described by a transfer matrix [8]:

$$
M_{4\times 4} = \begin{bmatrix} m_{11} & m_{12} & m_{13} & m_{14} \\ m_{21} & m_{22} & m_{23} & m_{24} \\ m_{31} & m_{32} & m_{33} & m_{34} \\ m_{41} & m_{42} & m_{43} & m_{44} \end{bmatrix}, \quad (1)
$$

where m_{ij} $(i, j = 1, \ldots, 4)$ are complex coefficients calculated by using the modal propagation method. At the length $L = \frac{3L_\pi}{4}$, the phases of the equal output signals at the output waveguides can be calculated from

$$
\phi_{ij} = \phi_0 + \pi + \frac{\pi}{16}(j - i)(8 - j + i), \text{ for } i + j \text{ even}
$$

$$
\text{and } \phi_{ij} = \phi_0 + \frac{\pi}{16}(i + j - 1)(8 - j - i + 1), \text{ for } i + j \text{ odd}.
$$

Here, input ports i $(i = 1, \ldots, 4)$ are numbered from down to up and the output ports j $(j = 1, \ldots, 4)$ are numbered from up to down in the MMI coupler and $\phi_0 = -\beta_0 L_{MMI} - \frac{\pi}{2}$ is a phase constant factor that is associated with the MMI ge-
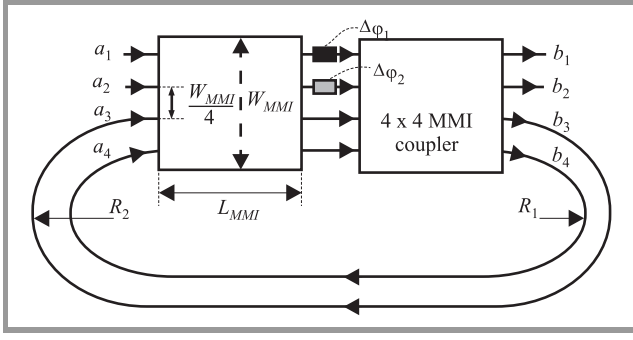
Fig. 1. The structure of a microring resonator based on 4×4 MMI couplers.

ometry and therefore can be neglected in the following analyses.

The 4×4 MMI coupler at a length of $L_1 = \frac{3L_\pi}{4}$ is described by the following transfer matrix:

$$M_{4 \times 4} = \frac{1}{2} \begin{bmatrix} -1 & -e^{j\frac{3\pi}{4}} & e^{j\frac{3\pi}{4}} & -1 \\ -e^{j\frac{3\pi}{4}} & -1 & -1 & e^{j\frac{3\pi}{4}} \\ e^{j\frac{3\pi}{4}} & -1 & -1 & -e^{j\frac{3\pi}{4}} \\ -1 & e^{j\frac{3\pi}{4}} & -e^{j\frac{3\pi}{4}} & -1 \end{bmatrix}. \quad (2)$$

If the length is doubled to $L_{MMI} = 2L_1 = \frac{3L_\pi}{2}$, a new 4×4 MMI coupler is formed and its transfer matrix is

$$M_{new} = (M_{4 \times 4})^2 = \frac{1}{2} \begin{bmatrix} 1-j & 0 & 0 & 1+j \\ 0 & 1-j & 1+j & 0 \\ 0 & 1+j & 1-j & 0 \\ 1+j & 0 & 0 & 1-j \end{bmatrix}. \quad (3)$$

This matrix can be considered as consisting of two separate submatrices which describe two 2×2 the 3 dB MMI couplers, both having the transfer matrix:

$$\mathbf{M_2} = \frac{1}{2} \begin{bmatrix} 1-j & 1+j \\ 1+j & 1-j \end{bmatrix} = \frac{1}{\sqrt{2}} e^{-j\frac{\pi}{4}} \begin{bmatrix} 1 & j \\ j & 1 \end{bmatrix}. \quad (4)$$

If two 4×4 MMI couplers are connected in the MZI structure of Fig. 1, then the relations between the complex amplitudes at the input ports and output ports can be expressed in terms of the transfer matrices of the 3 dB MMI couplers and the phase shifters as follows:

$$\begin{bmatrix} b_1 \\ b_2 \end{bmatrix} = e^{j\frac{\Delta\varphi_1}{2}} \begin{bmatrix} \tau_1 & \kappa_1 \\ \kappa_1^* & -\tau_1^* \end{bmatrix} \begin{bmatrix} a_1 \\ a_2 \end{bmatrix}, \quad (5)$$

where $\tau_1 = \sin(\frac{\Delta\varphi_1}{2})$ and $\kappa_1 = \cos(\frac{\Delta\varphi_1}{2})$, $\quad (6)$

$$\begin{bmatrix} B_1 \\ B_2 \end{bmatrix} = e^{j\frac{\Delta\varphi_2}{2}} \begin{bmatrix} \tau_2 & \kappa_2 \\ \kappa_2^* & -\tau_2^* \end{bmatrix} \begin{bmatrix} A_1 \\ A_2 \end{bmatrix}, \quad (7)$$

where $\tau_2 = \sin(\frac{\Delta\varphi_2}{2})$ and $\kappa_2 = \cos(\frac{\Delta\varphi_2}{2})$. $\quad (8)$

Therefore, the whole device can be viewed as consisting of two independent microresonators having different power coupling ratios as shown in Fig. 2. This means that two independent switches and filters can be made by using this structure.
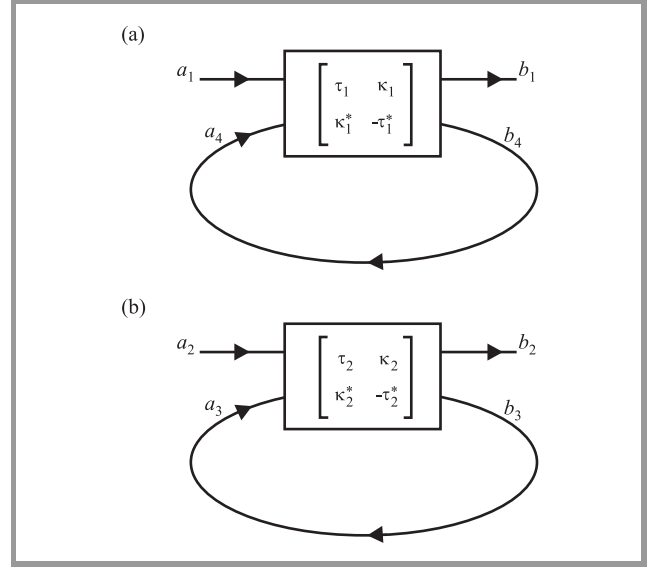

Fig. 2. Two separate microresonators created from the 4×4 MMI structure: (a) microresonator using input ports 1 and 4, and (b) microresonator using input ports 2 and 3.
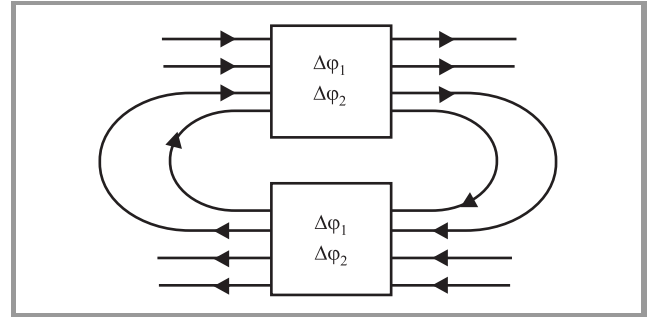

Fig. 3. Two separate add-drop multiplexers based on microresonators using 4×4 MMI-MZI structures.

Another useful structure for implementing add-drop multiplexing functions is shown in Fig. 3, where the microresonator is coupled to a second MMI-MZI structure. The coupling ratios can be controlled by the phase shifters. Similarly, two independent add-drop filters can be obtained from this structure.

3. Simulation Results and Discussions

In this section, in order to verify the working principle of the devices, the three dimensional beam propagation method (3D-BPM) [9], [10] is used to optimize the designs for MMI devices. It is well known that the finite difference time-domain (FDTD) method is a general method

to solve Maxwell's partial differential equations numerically in the time domain. Simulation results for devices on the SOI channel waveguide using the 3D-FDTD method can achieve a very high accuracy. However, due to the limitation of computer resources and memory requirements, it is difficult to apply the 3D-FDTD method to the modeling of large devices on the SOI channel waveguide. Meanwhile, the 3D-BPM was shown to be a quite suitable method [11], [12] that has sufficient accuracy for simulating devices based on SOI channel waveguides [13], [14].

The waveguide structure used in the designs is shown in Fig. 4. Here, SiO_2 ($n = 1.46$) is used as the upper cladding material. An upper cladding region is needed for devices using the thermo-optic effect in order to reduce loss due to metal electrodes. Also, the upper cladding region is used to avoid the influence of moisture and environmental temperature.
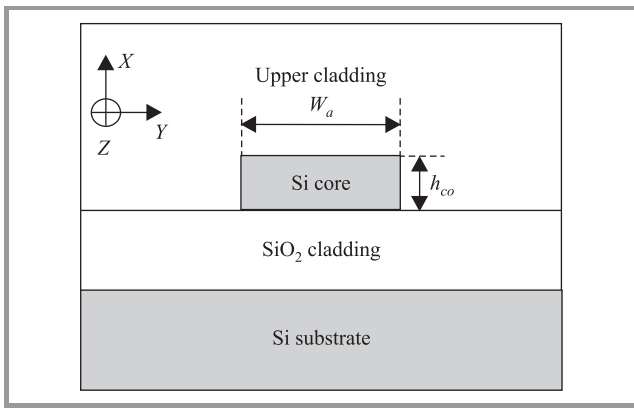

Fig. 4. Waveguide structure used in the simulations.

The parameters used in the designs are as follows: the waveguide has a standard silicon thickness of $h_{co} = 220$ nm and access waveguide widths are $W_a = 0.48$ μm for single mode operation. The refractive index of the silicon core is $n_{Si} = 3.45$. It is assumed that the designs are for the TE (transverse electric) polarization at a central optical wavelength $\lambda = 1550$ nm. The width of the MMI is $W_{MMI} = 6$ μm. The access waveguide is tapered to a width of $W_{tp} = 800$ nm to improve device performance.

The 3D-BPM simulations for a 4×4 MMI coupler having a length of $L_1 = \frac{3L_\pi}{4}$ are shown in Fig. 5a for a signal presented at input port 1 and Fig. 5b for a signal at input port 2. The optimized length of the MMI coupler calculated by using 3D-BPM is $L_1 = 71.70$ μm. The excess loss calculated is 0.35 dB for both cases.

If two 4×4 MMI couplers with the same length of $L_{MMI} = \frac{3L_\pi}{4}$ are cascaded together, then a 4×4 MMI coupler having a length of $L_{MMI} = \frac{3L_\pi}{2}$ is formed. The transfer matrix of this new 4×4 MMI coupler is given by Eq. (4). The 3D-BPM will now be used to verify this prediction. The 3D-BPM simulations for this 4×4 MMI coupler are shown in Fig. 6. The 3D-BPM simulations show that the power splitting ratios for each MMI coupler used in these microresonators are 0.42/0.43. The optimized length of
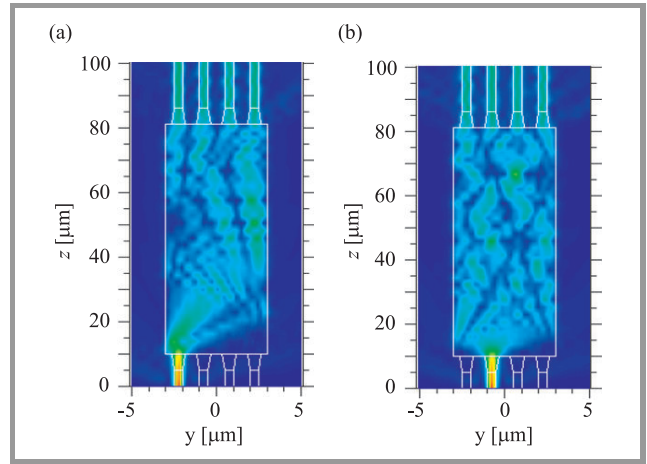

Fig. 5. The 3D-BPM simulations for a 4×4 MMI coupler at length $L_1 = \frac{3L_\pi}{4}$ with input signal at (a) port 1 and (b) port 2.
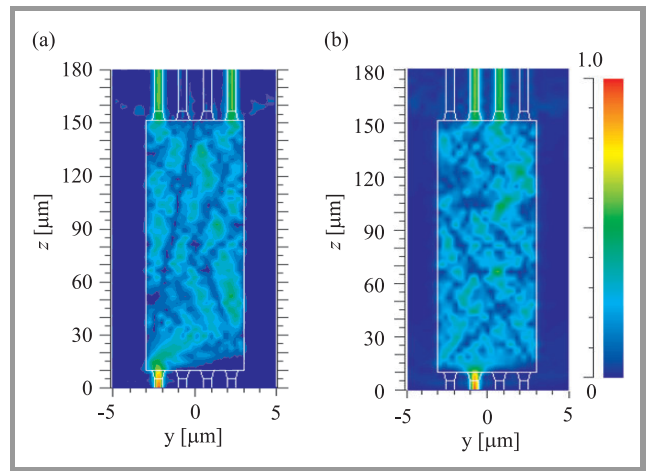

Fig. 6. The 3D-BPM simulations for a 4×4 MMI structures with the signal at (a) input port 1 and (b) input port 2.

each MMI coupler is found to be $L_{MMI} = 141.7$ μm. For both cases, the excess losses are 0.7 dB and the imbalances are 0.1 dB.

By connecting the above MMI structures (each MMI with length of $L_{MMI} = \frac{3L_\pi}{2}$) together as shown in Fig. 1, double-microresonators can be achieved. Phase shifters can be introduced in the linking arms of the MZI structure in order to vary the coupling coefficients of the couplers. For example, if phase shifts of $\Delta\varphi_1 = \Delta\varphi_2 = 0$ are introduced at the linking arms of the MZI, then the 3D-BPM simulation (Fig. 7a) shows that the normalized output powers (for signal at input port 1) at output ports 1, 2, 3 and 4 are 0, 0, 0 and 0.8, respectively. The computed excess loss is 0.96 dB.

If phase shifts $\Delta\varphi_1 = \frac{\pi}{2}$ and $\Delta\varphi_2 = 0$ are introduced at the linking arms, the 3D-BPM simulation for the signal at input port 1 is shown in Fig. 7b. The normalized output powers at output ports 1, 2, 3 and 4 calculated to be 0.41, 0, 0 and 0.39, respectively. The excess loss is 0.9 dB and the imbalance is 0.2 dB in this case.
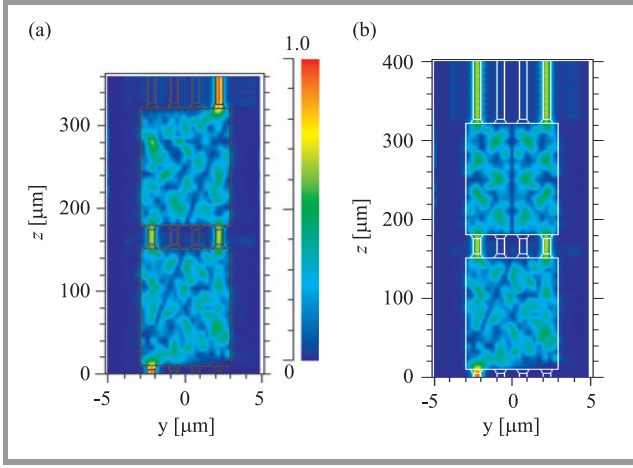
Fig. 7. The 3D-BPM simulations of cascaded MMI couplers used for the microresonator structure when the signal is at input port 1 with (a) phase shifts $\Delta\varphi_1 = \Delta\varphi_2 = 0$ and (b) $\Delta\varphi_1 = \frac{\pi}{2}$ and $\Delta\varphi_2 = 0$.

The quality factor (Q) of a single microresonator based on a 2×2 MMI coupler is given by [2]

$$Q \approx \frac{\pi n_g L_R \sqrt{\alpha\tau}}{\lambda(1 - \alpha\tau)}. \qquad (9)$$

Here, n_g, L_R, and λ are the group index, length of the racetrack waveguide and wavelength, respectively. τ is the transmission coefficient of the coupler. In order to achieve a high Q microresonator, the coupling coefficient $|\kappa| = \sqrt{\alpha^2 - \tau^2}$ needs to be small. Note that the bend radius also has a strong effect on the Q-factor. However, if the bend radius increases, then the transmission loss will increase, while the bend loss does not significantly decrease. Here α^2 is the power loss factor introduced by MMI couplers and racetrack waveguides (including both bend loss and transmission loss). By varying the phase shifts at the linking arms, the power coupling ratios can be tuned.

The complete device presented in this paper is equivalent to two separate 2×2 MMI-based microresonators. Each microresonator may have different transmission characteristics such as different quality (Q), different free spectral range (FSR), finesse (F) and different bandwidth (BW).

In the following examples, the Q-factors of the microring resonators will be determined. Consider a 4×4 microring resonator with following parameters: bend radii of the first microring resonator and second microring resonator (see Fig. 1) are $R_1 = 5$ μm and $R_2 = 20$ μm. If the 3 dB MMI couplers with the same length of ($L_{MMI} = 141.7$ μm (Fig. 6) are used in the structure, then the calculated power transmission coefficients are $|\tau_1|^2 = 0.42$ and $|\tau_2|^2 = 0.42$. The estimated Q-factor for the first microring resonator is $Q_1 \approx 1000$ and for the second microring resonator is $Q_2 = 1650$.

If two 4×4 MMI couplers having the same length of $L_{MMI} = 141.7$ μm are connected together in order to produce 2×2 tunable MMI couplers (Fig. 7), then power transmission ratios of the two MMI couplers $|\tau_1|^2$ and $|\tau_2|^2$

can be varied by adjusting the phase shifts $\Delta\varphi_1$ and $\Delta\varphi_2$ in the linking arms, respectively. For example, if phase shifts $\Delta\varphi_1 = 0.9\pi$ and $\Delta\varphi_2 = 0.5\pi$, then the 3D-BPM shows that the normalized output powers at output ports 1, 2, 3 and 4 are 0.7, 0, 0 and 0.1, respectively. The calculated power transmission coefficients are $|\tau_1|^2 = 0.7$ and $|\tau_2|^2 = 0.41$. Therefore, the estimated Q-factors are $Q_1 \approx 4300$ for the first microring resonator with bend radius $R_1 = 5$ μm and $Q_2 \approx 2500$ for the first microring resonator with bend radius $R_2 = 20$ μm.

It is interesting to note that provided that the phase shifters operate with sufficient speed, functions of switching, modulating and add-drop multiplexing can be achieved in both microresonators.

4. Conclusions

In this paper, we have presented a novel microring resonator structure based on 4×4 MMI couplers. This device acts as two separate microring resonators. The design of the device on the SOI platform has been presented by using the transfer matrix method and the working principle is verified using the 3D BPM method. If the phase shifters operate fast enough, then the device may be a very promising building block for optical switches, optical modulators, and optical add-drop multiplexers.

References

[1] D. G. Rabus, *Integrated Ring Resonators – The Compendium*. Berlin: Springer-Verlag, 2007.

[2] D.-X. Xu, A. Densmore, P. Waldron, J. Lapointe, E. Post, and A. Delâge, "High bandwidth SOI photonic wire ring resonators using MMI coupler", *Opt. Expr.*, vol. 15, no. 6, pp. 3149–3155, 2007.

[3] F. Xia, L. Sekaric, and Y. A. Vlasov, "Mode conversion losses in silicon-on-insulator photonic wire based racetrack resonators", *Opt. Expr.*, vol. 14, no. 9, pp. 3872–3886, 2006.

[4] T. T. Le and L. W. Cahill, "The modeling of MMI structures for signal processing applications", in *Integr. Opt. Dev. Mater. Technol. XII Proc. SPIE*, San Jose, USA, 2008, vol. 6896, pp. 68961G–68961G-7.

[5] P. A. Besse, E. Gini, M. Bachmann, and H. Melchior, "New 2×2 and 1×3 multimode interference couplers with free selection of power splitting ratios", *IEEE J. Lightw. Technol.*, vol. 14, no. 10, pp. 2286–2293, 1996.

[6] A. Yariv, "Critical coupling and its control in optical waveguide-ring resonator systems", *IEEE Photon. Technol. Lett.*, vol. 14, no. 4, pp. 483–485, 2002.

[7] J. M. Choi, R. K. Lee, and A. Yariv, "Control of critical coupling in a ring resonator-fiber configuration: application to wavelength-selective switching, modulation, amplification, and oscillation", *Opt. Lett.*, vol. 26, no. 16, pp. 1236–1238, 2001.

[8] M. Bachmann, P. A. Besse, and H. Melchior, "General self-imaging properties in $N \times N$ multimode interference couplers including phase relations", *Appl. Opt.*, vol. 33, no. 18, pp. 3905–3911, 1994.

[9] W. P. Huang, C. L. Xu, and S. K. Chaudhuri, "A finite-difference vector beam propagation method for three-dimensional waveguide structures", *IEEE Photon. Technol. Lett.*, vol. 4, no. 2, pp. 148–151, 1992.

[10] W. P. Huang, C. L. Xu, W. Lui, and K. Yokoyama, "The perfectly matched layer (PML) boundary condition for the beam propagation method", *IEEE Photon. Technol. Lett.*, vol. 8, no. 5, pp. 649–651, 1996.

[11] D. Dai and S. He, "Design of an ultrashort Si-nanowaveguide-based multimode interference coupler of arbitrary shape", *Appl. Opt.*, vol. 47, no. 19, pp. 38–44, 2008.

[12] D. Dai and S. He, "Optimization of ultracompact polarization-insensitive multimode interference couplers based on Si nanowire waveguides", *IEEE Photon. Technol. Lett.*, vol. 18, no. 19, pp. 2017–2019, 2006.

[13] E. Dulkeith *et al.*, "Group index and group velocity dispersion in silicon-on-insulator photonic wires", *Opt. Expr.*, vol. 14, no. 9, pp. 3853–3863, 2006.

[14] J. I. Dadap *et al.*, "Nonlinear-optical phase modification in dispersion-engineered Si photonic wires", *Opt. Expr.*, vol. 16, no. 2, pp. 1280–1299, 2008.
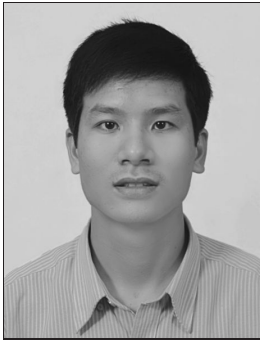
Trung-Thanh Le received the B.E. and M.E. degrees in electronic and telecommunication engineering from the Hanoi University of Technology, Vietnam, in 2003 and 2005, respectively. Since 2003, he has been a lecturer at the National University of Transportation and Communications, Hanoi. He works towards the Ph.D. degree in electronic engineering at the La Trobe University, Melbourne, Australia, since 2006. His research interests are integrated optical devices and photonic signal processing, especially multimode interference based devices.
e-mail: thanh.latrobe@gmail.com
Department of Electronic Engineering
La Trobe University
Melbourne, Vic 3086, Australia
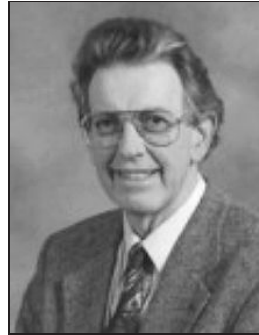
Laurence W. Cahill received the B.E., M.Sc. and Ph.D. degrees from the University of Melbourne, Australia. He is a Professor in the Department of Electronic Engineering, La Trobe University, Australia. He is a senior member of the IEEE, member of SPIE and a Fellow of Engineers Australia. His research interests lie in the area of optical and photonics. Particular interests are semiconductor laser dynamics, high speed circuits for optical sources and receivers, mid infrared detectors, photonic switching, fibre sensors, computer aided design, image processing, and signal processing.
e-mail: L.Cahill@latrobe.edu.au
Department of Electronic Engineering
La Trobe University
Plenty road, Bundoora Campus
Melbourne, Vic 3086, Australia